COUPLED SIMULATIONS OBTAINED WITH THE UCLA AGCM WITH A NEW PBL PARAMETERIZATION AND THE MIT GLOBAL OGCM

Gabriel Cazes Boezio[1,4], Celal S. Konor[2], Carlos R. Mechoso[1], Dimitris Menemenlis[3] and Akio Arakawa[1]

[1] Department of Atmospheric Sciences, University of California Los Angeles, California

[2] Department of Atmospheric Science, Colorado State University, Colorado

[3] NASA/Caltech Jet Propulsion Laboratory, Pasadena, California

[4] On leave from IMFIA, Universidad de la Republica, Uruguay

1. Introduction

The quality of simulated surface fluxes of momentum, latent and sensible heat, and water vapor mass exchanged between the atmosphere and the underlying surface are of crucial importance for atmospheric general circulation models (AGCMs), particularly when they are coupled to ocean or soil models. In AGCMs these fluxes are provided by the parameterization of planetary boundary layer (PBL) processes. The PBL parameterization also provides boundary layer cloudiness, which strongly influences the surface radiation fluxes and hence the predicted SSTs in coupled atmosphere-ocean simulations (Ma et al. 1996, Mechoso et al. 2000).

This paper presents a coupled simulation by a version of the UCLA AGCM with a revised PBL parameterization, coupled to the MIT ocean general circulation model (OGCM). A new PBL parameterization has been implemented and tested in the UCLA AGCM (Konor et al. 2004). As in other versions of the UCLA AGCM (Suarez et al. 1983), the sigma-type vertical coordinate shares a coordinate surface with the free atmosphere at the PBL-top. This framework facilitates an explicit representation of processes concentrated near the PBL top, which is crucial for predicting PBL clouds. A novel feature is the definition of multiple layers between the PBL top and the earth surface. This allows for explicit prediction of the vertical profiles of potential temperature, water mixing ratio and horizontal wind vectors in the PBL. Also the new parameterizaton predicts the bulk (vertically integrated) turbulent kinetic energy (TKE), following Randall and Schubert (2004). TKE is used for the computation of the surface fluxes of moisture, sensible heat and momentum. TKE is also used for an explicit formulation of the mass entrainment rate at the PBL top, which also follows Randall and Schubert (2004). The AGCM used for the coupled simulation presented in this work is in an intermediate stage of development and uses the new formulation of surface fluxes and mass entrainment rate at the PBL top, but the PBL is considered as well-mixed.

In section 2 of this paper we describe general aspects of the UCLA AGCM and the parameterization of the PBL processes. In section 3 we show results of a simulation with prescribed SST. In section 4 we discuss the results and present our conclusions.

2. Model description.

The UCLA AGCM is a finite difference model that integrates the primitive equations of the atmosphere. The model's horizontal discretization is arranged as a "C grid"; the vertical discretization is arranged as a Lorenz grid. The parameterizations of the major physical processes include solar and terrestial radiation calculations according to Harshvandan et al. (1987 and 1989, respectively), and the cumulus convection scheme by Arakawa and Schubert (1974), as revised by Pan and Randall (1994).

The PBL Parameterization.

TKE is predicted according to equations (8.3) to (8.6) in Konor and Arakawa (2005). The surface fluxes of momentum, temperature and moisture are determined from an aerodynamic formula based on Deardorff (1972). Our formulation considers both the square root of the bulk TKE and the mean large-scale PBL velocity to determine the velocity scale. This formulation of the surface fluxes is expected to provide better estimates than the traditional methods, since the mean surface wind can be weak while the convective mixing is strong. The surface fluxes of momentum, temperature and moisture are computed as follows:

$$\left.\begin{aligned} F_v &= \rho_s C_U C_U \max\left(\alpha_1 u_M , \beta_1 \sqrt{e_M}\right)\mathbf{v}_M \\ F_\theta &= \rho_s C_U C_T \max\left(\alpha_2 u_M , \beta_2 \sqrt{e_M}\right)(\theta_G - \theta_M) \\ F_q &= \rho_s C_U C_T \max\left(\alpha_2 u_M , \beta_2 \sqrt{e_M}\right)(q_G - q_M)\, k \end{aligned}\right\}$$

where ρ_s is air density at the Earth's surface, and C_U and C_T are coefficients that depends on the bulk Richardson number, the PBL thickness and the surface roughness length, and are computed as in Deardorff (1972). u_M e_M, v_M, θ_M and q_M are, respectively, the module of the velocity, the TKE, the vector velocity, the potential temperature and the moisture at the PBL. θ_G is the earth surface potential temperature, and q_G is the saturation moisture at the earth surface temperature and pressure. k is a coefficient of water availability of the terrain. This coefficient is one in water surfaces, and close to zero in arid terrains. α_1, α_2, β_1 and β_2 are empirical scale coefficients. The turbulent mass entrainment at the PBL top is computed according to equations (8.12), (8.14) and (8.27) in Konor and Arakawa (2005).

The MIT OGCM.

The MIT OGCM is described in Marshall et al. (1997). The model employs the K-Profile Parameterization (KPP) vertical mixing scheme of Large et al. (1994) and the isopycnal mixing schemes of Redi (1982) and Gent and McWilliams (1990), with surface tapering as in Large et al. (1997). At the bottom and lateral boundaries no-slip and free-slip conditions are applied, respectively. At the top, a free surface condition is applied.

3. Results of a coupled simulation

In this section we examine selected results from a 35-years long simulation that was started with atmospheric and oceanic conditions corresponding to January 10th in long uncoupled simulations. The horizontal resolution used for the UCLA AGCM was 5º in longitude by 4º degrees in latitude and there are 14 vertical layers in the free atmosphere and one in the PBL. The MIT OGCM domain spans the latitudes 80ºS to 79ºN. In the zonal direction the resolution is 1º. In the meridional direction, the resolution is 0.3º within 10º of the equator, increasing to 1º outside the tropics. There are 46 levels in the vertical, with thicknesses ranging from 10 to 400m. We present monthly and annual means of several simulated fields averaged through the last 30 years of the simulation, since the first years may be affected by adjustment to the model climatology.

Figure 1 shows the simulated January and July mean sea level pressure (SLP, Figs. 1a and 1c) and the respective climatologies derived from the NCEP reanalysis (Figs. 1b and 1d). We find that the simulation captures many outstanding features of the observed climatology, such as the Aleutian low in the Northern Hemisphere winter, the subtropical anticyclones over the northern oceans during summer, and the subtropical belt of high pressures in the Southern Hemisphere, although the latter is weaker than the observed. Figure 2 shows the simulated January and July mean precipitation (Figs. 2a and 2c), and the respective climatologies derived from the Arkin-Xie analysis (Figs. 2b and 2d). The simulated global patterns are comparable with the analysis. However, the simulated precipitation is weaker in the ITCZs and the South American and African monsoon regions. We also find that the simulated precipitation in the southern tropical Pacific and Atlantic extends further eastward than in the Arkin-Xie analysis.

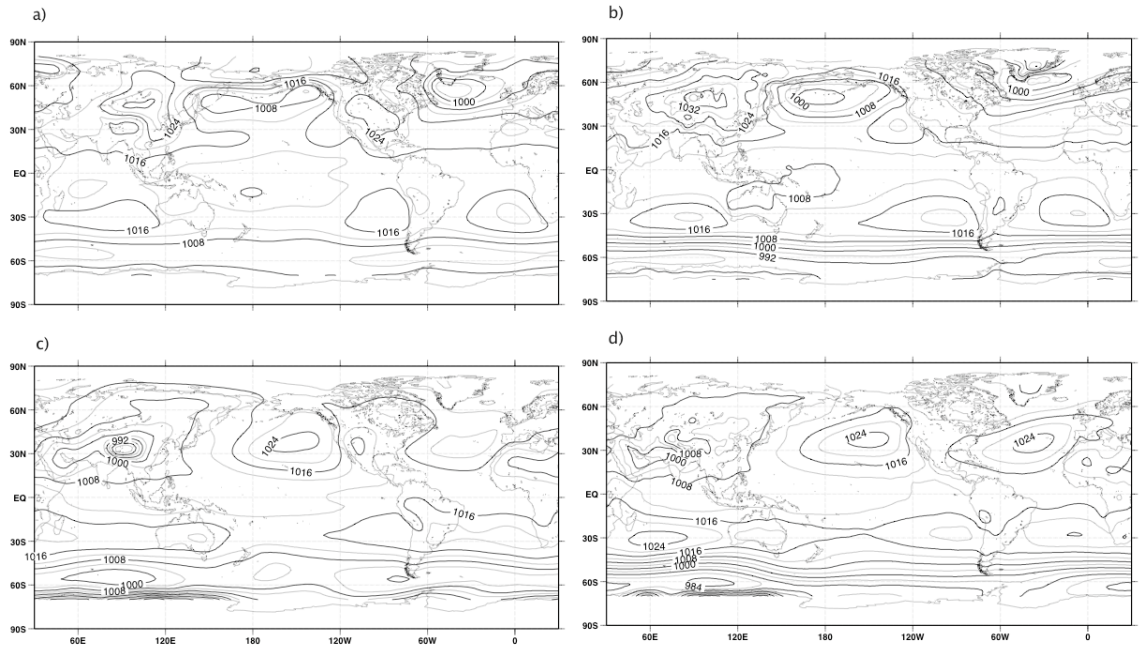

Fig. 1 a) Simulated January mean SLP. b) January mean SLP according to NCEP reanalysis. c) Same as a), except for July. d) Same as b), except for July. Contour interval is 4 hPa.

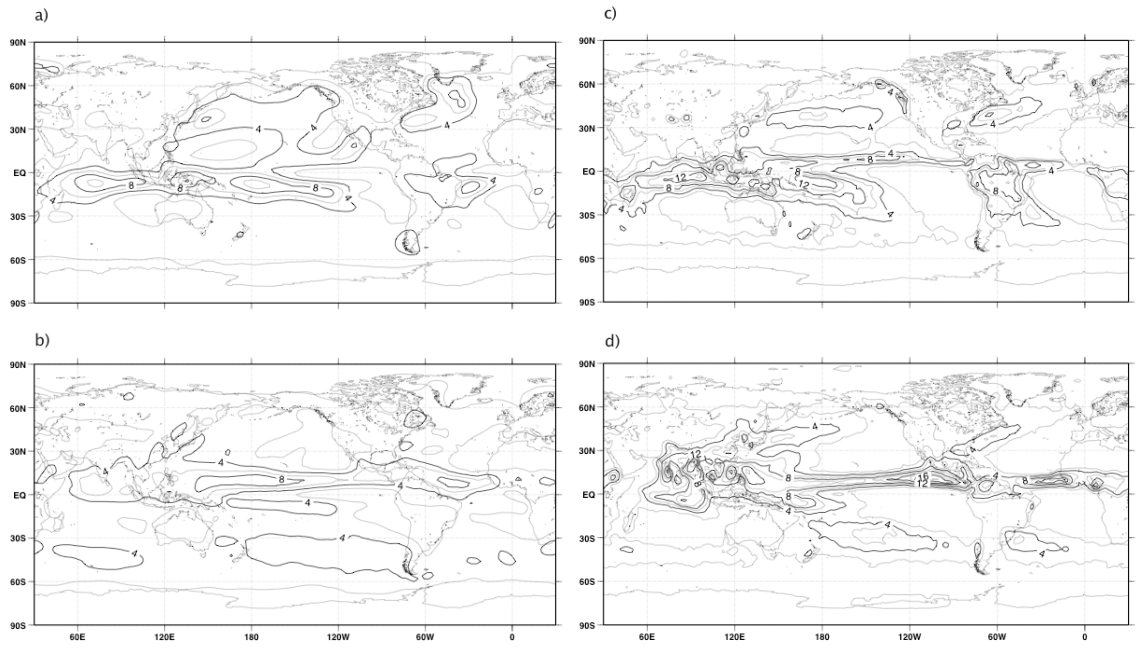

Fig. 2 a) Simulated January mean precipitation. b) January mean precipitation according to Arkin-Xie analysis. c) Same as a), except for July. d) Same as b), except for July. Contour interval is 2 mm/day.

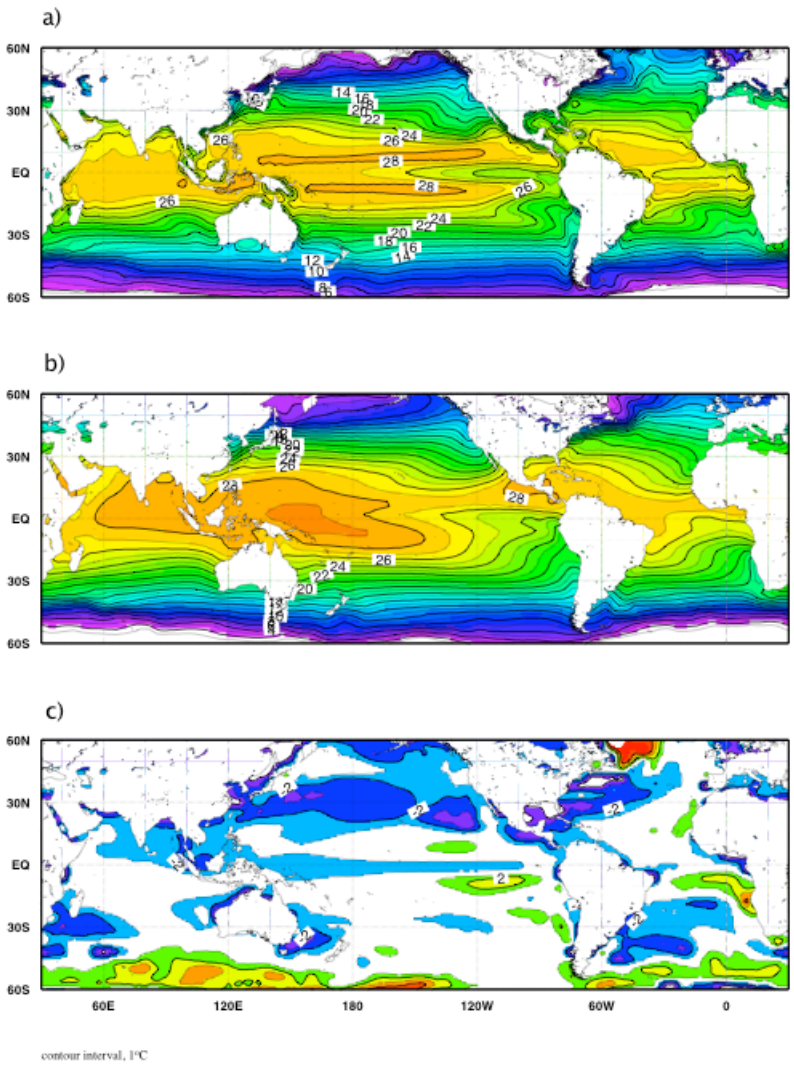

Fig 3. a) Simulated annual mean SST. b) Annual mean SST according to Reynolds analysis. c) Difference between a) and b). Contour interval is 1°C.

Figure 3 shows the simulated annual mean SST distribution (Fig. 3a), the climatological annual mean SST according to the Reynolds analysis (Fig. 3b) and the difference between simulated and analyzed fields (Fig. 3c). The simulated zonal SST gradient in the equatorial Pacific is about 4°C, which is comparable to that in the observations (about 5°C). The simulation reproduces the cold tongue in the tropical eastern Pacific, and captures its asymmetry respect to the equator. In the equatorial Atlantic, the zonal SST gradient is about half of the observed, although at least has the correct sign. At the tropical southern Pacific and Atlantic Oceans, the simulated warm pool extends too much to the east, as was also found with the precipitation. The model, therefore, shares with others the simulation of a spurious double ITCZ (Mechoso et al. 1995). Also the simulated SST at the equatorial Pacific are about 1°C colder than

at the analysis. On the other hand, the errors along the eastern coasts of the tropical oceans are very small. The coupled model, therefore, achieves a rare success in the simulation of marine stratocumulus.

Figure 4 shows a vertical section of the annual mean temperature at the equator in the Pacific Ocean. Only the upper 400m are shown. The figure shows that the thermocline is about 150 to 200 meters deep in the western Pacific, while it is near the surface in the east. These are realistic features of the thermocline climatology.

Figure 5 shows the mean annual cycle of SST at the equator in the Pacific for the simulation (Fig. 5a) and the Reynolds analysis (Fig. 5b). Fields are presented as Hovmuller diagrams that show, at each longitude and each month, the departure of the monthly mean vale from the annual mean at that particular longitude. The simulated annual cycle has weaker amplitude than the observed one. The simulation has maximum SST departures from the annual mean in the eastern Pacific around April, as in the observations. However, the simulated eastern Pacific SSTs also shows a secondary maximum around November, and minima around July-August and January. Therefore, the simulated annual cycle of the equatorial Pacific SSTs in the simulation has a semiannual component that is stronger than in the observations.

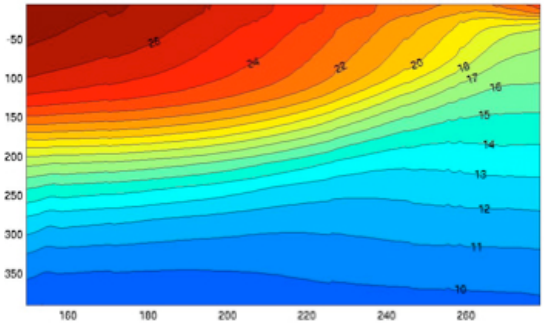

Fig. 4. Simulated annual mean temperature at the upper 400 m of the Pacific Ocean at the equator. Contour interval is 1°C.

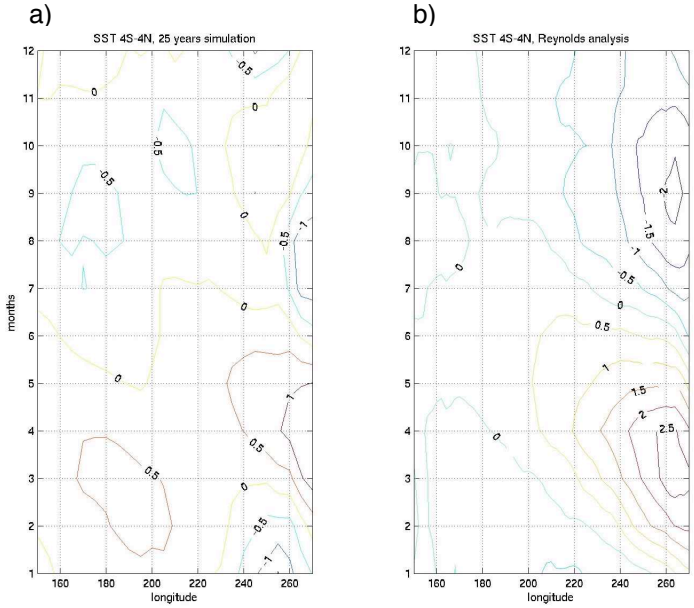

Fig. 5. a) Hovmuller diagram of the simulated monthly mean SSTs at the Pacific Ocean, averaged between 4°S-4°N. The annual mean at each longitude was substracted. b) Same as a), except for the climatological monthly means according to the Reynolds analysis. Contour interval is 0.5°C.

Next we focus on simulated fields that are directly affected by the PBL parameterization. Figure 6 shows simulated monthly means of stratocumulus clouds incidence, defined as percentage of time of occurrence, for January (Fig. 6a), April (Fig. 6b), July (Fig. 6c) and October (Fig. 6d). We can see areas of relative high values off the coasts of California, Peru, and Namibia. There is also a relative high incidence of stratocumulus clouds in the storm track regions. These features are consistent with analysis from observations (e.g. Klein and Hartman 1993). The maximum and minimum stratocumulus incidence off Peruvian and Namibian coasts occur in October and April, which is consistent with Hartman and Klein (1993) analysis. The value of incidence, however, is a little too high during January and too small during July.

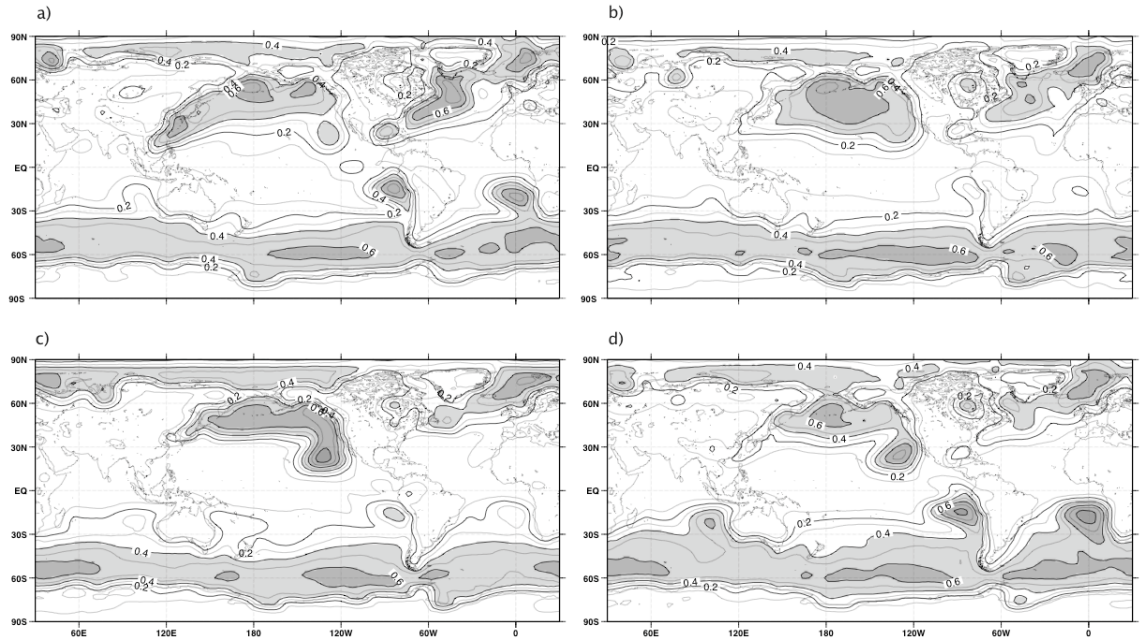

Fig. 6 Simulated monthly mean stratocumulus clouds incidence for a) January, b) April, c) July, and d) October. Contour interval is 0.1.

Figure 7 shows the simulated January and July mean short wave radiation at the Earth's surface (Figs. 7a and 7c) and the corresponding fields derived from the NASA SRB analysis (Figs. 7b and 7d). Figure 8 shows the simulated January and July mean latent heat flux at the Earth's surface (Figs. 8a and 8c) and the corresponding fields derived from COADS analysis (Figs. 8b and 8d). The simulated short wave radiation fluxes are very similar to those of the NASA SRB analysis, while latent heat flux in the tropical oceans is about 20 to 30 Watts/m^2 stronger than the COADS data.

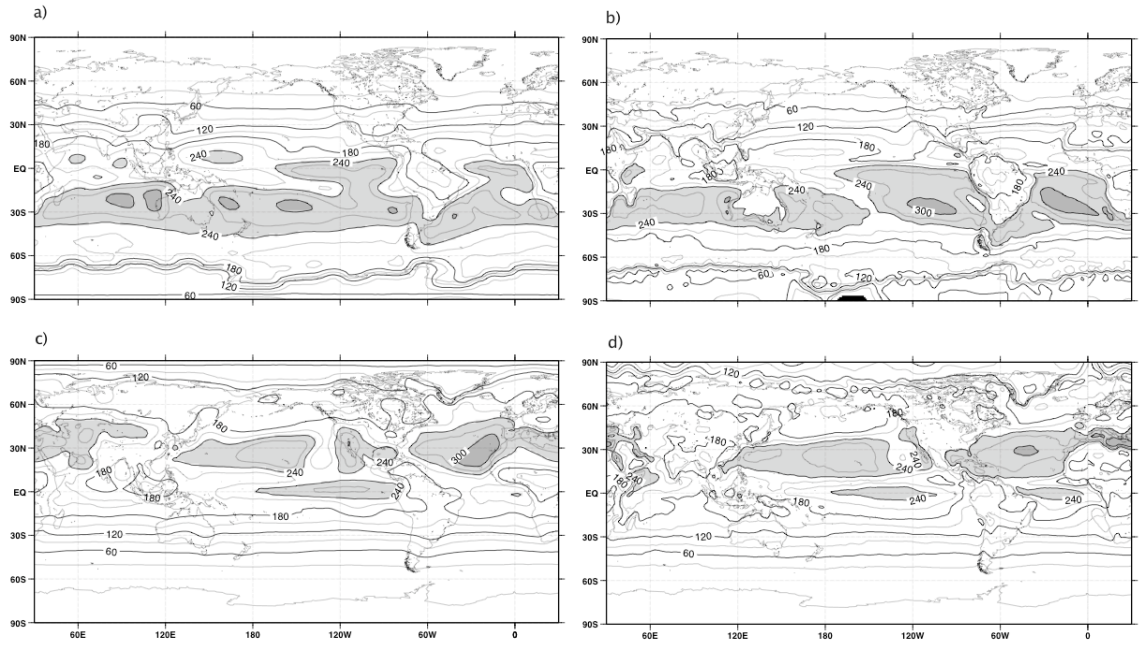

Fig. 7 a) Simulated January mean short wave radiation at Earth's surface. b) Short wave radiation at Earth's surface derived from the NASA SRB analysis for the Januarys (1983 to 1992). c), d) Same as a) and b) respectively, except for July. Contour interval is 30 Watts/m^2.

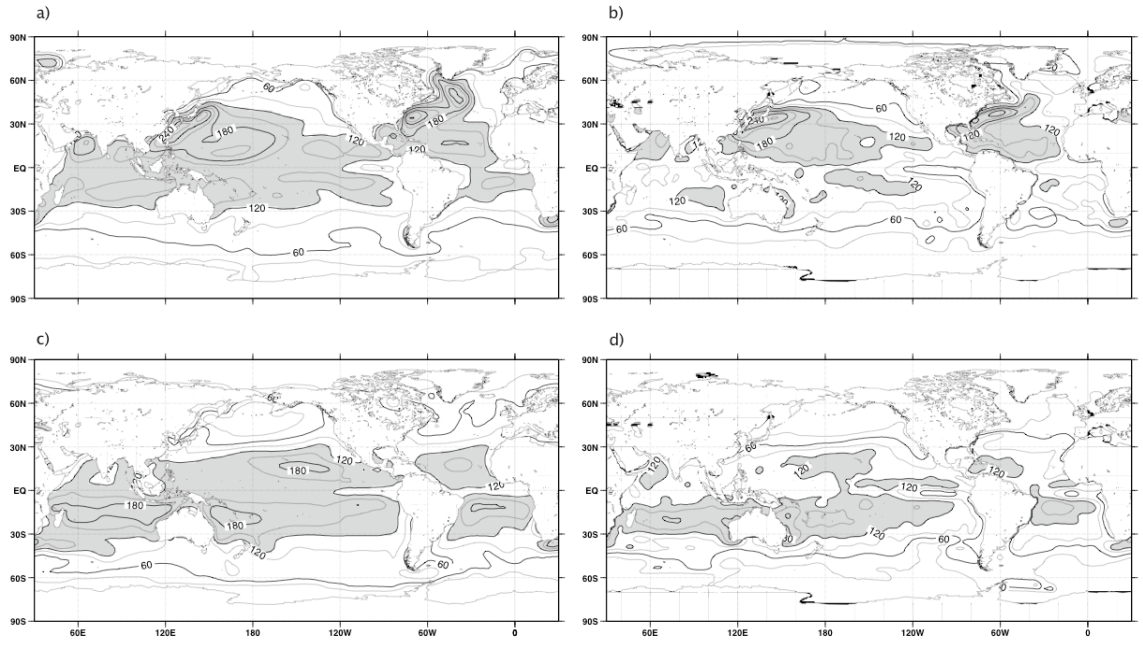

Fig. 8. a) Simulated January mean latent heat flux at Earth's surface. b) Latent heat flux at Earth's surface derived from the COADS analysis the January (1979 to 1992). c), d) Same as a) and b) respectively, except for July. Contour interval is 30 Watts/m^2.

The simulated wind stresses at Earth's surface (not shown) have a realistic geographical pattern compared with the climatology derived from COADS analysis. However, the simulated wind stresses are weaker, about 2/3 than those obtained from the analysis.

In order to have a preliminary assessment of the simulated interannual variability at the equatorial Pacific, we present in Fig. 9 a Hovmuller diagram of monthly mean SST anomalies (Fig. 9a) and zonal wind stress anomalies (Fig. 9b) averaged between 4ºS and 4ºN. Figure 9 shows ENSO-like anomalies. As in the observations, the maximum and minimum SST anomalies appear in the eastern Pacific during the Northern Hemisphere winter. The simulated ENSO-like signal in the 30 years run has a period between 3 to 7 years and an amplitude of 2º to 3º C. The zonal wind stress diagram shows weaker and stronger trade winds associated with the warm or cold SST anomalies respectively. Also the simultaneous correlation between simulated SST at Niño 3 region (5ºS–5ºN, 90ºW–150ºW) and simulated SLP during November-December (Fig. 10a) is comparable with the Southern Oscilation pattern computed from observations (Fig. 10 b).

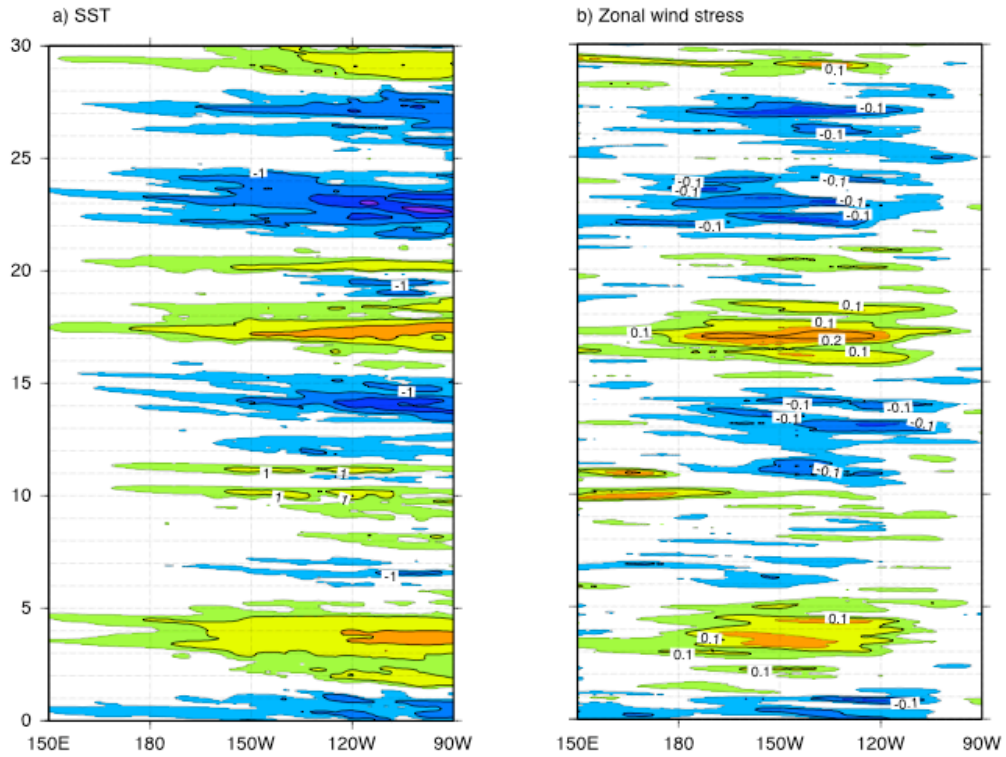

Fig 9 a) Hovmuller diagram of monthly mean SST anomalies for the last 30 years of the simulation, averaged between 4ºS-4ºN, in the equatorial Pacific. Contour interval is 1ºC, +/- 0.5ºC contours are also shown. b) Same as a), except for monthly mean zonal wind stress anomalies. Contour interval is 0.05 dyn/cm^2.

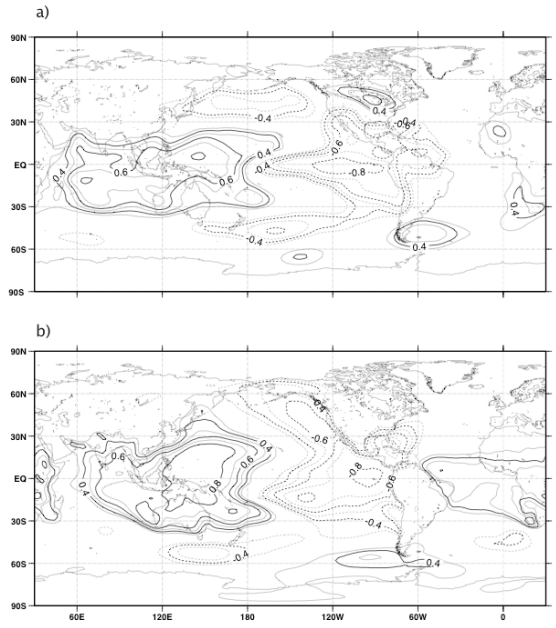

Fig. 10 a): Simultaneous correlations between simulated SST in the Niño 3 region and simulated SLP during November-February. b): Same as a), except derived from observations (Reynolds analysis for SST and NCEP reanalysis for SLP). Contour interval is 0.1; only values above 0.3 and below –0.3 are shown.

4. Summary and Conclusions

We have presented selected results from a coupled simulation by the UCLA AGCM coupled the global MIT OGCM. The AGCM includes features of a new PBL parameterization (Konor and Arakawa 2005), which maintains some advantages of the one developed by Suarez et al. (1983) and used in previous model versions. In particular, the definition of the σ coordinate makes the PBL top a coordinate surface, which allows for explicit computation of discontinuities at the PBL top and a more direct account of their effects. The entrainment formulas are explicit and make use of the PBL TKE. The bulk aerodynamic formulas for the computation of the surface fluxes use both the mixed layer mean velocity and the TKE.

The results of the coupled simulation are very encouraging. The simulated SLP and precipitation have several realistic features. Errors in heat fluxes at the sea surface are much smaller, compared to the observation, than in previous versions of the UCLA AGCM (i.e. Yu and Mechoso 1999). The simulated SST field shows a reasonable zonal gradient along the equatorial Pacific, and it has the correct sign along the equatorial Atlantic. Interannual variability of SST at the equatorial Pacific and the corresponding variability of the equatorial wind stress and SLP show ENSO-like events. There is, however, a spurious double ITCZ in the southern tropical Pacific and Atlantic Oceans. There is also an unrealistically strong semiannual component in the annual cycle of the equatorial Pacific SST as well as in the annual cycle of stratus incidence off Peruvian and Namibian coasts. Wind stresses tend to be weaker than those derived from the COADS analysis, although their geographical pattern is realistic.

The performance of this coupling model is encouraging. The examination of the impact on the simulations of a multilayer PBL and the reasons for the unrealistic features found so far have high priority in our current research.

Aknowledgements: This research was supported by NASA CAN 21425/041, NOAA Grant NA030AR4310095, the Department of Energy, Grant DE-FG 02-04ER63848, Department of Energy Cooperative Agreement FG-02-01ER63163, Colorado State University Contract G-3816-3, and NSF Grant ATM0071345.

References

Arakawa, A., and W. H. Schubert, 1974: Interaction of a cumulus cloud ensemble with the large-scale environment, Part I. *J. Atmos. Sci.*, **31**, 674-701.

Arakawa, A., and M. J. Suarez, 1983: Vertical differencing of the primitive equations in sigma coordinate. *Mon. Wea. Rev.*, **111**, 34-45.

Harshvardhan, R. Davies, D. A. Randall and T. G. Corsetti, 1987: A fast radiation parameterization for atmospheric circulation models. *J. Geophys., Res.*, **92**, 1009-1016.

Harshvardhan, D. A. Randall, T. G. Corsetti, and D. A. Dazlich, 1989: Earth radiation budget and cloudiness simulations with a

general circulation model. *J. Atmos. Sci.*, **46**, 1922-1942.

Klein S. A.,.D. L. Hartmann, 1993: The seasonal cycle of low stratiform clouds, *J. Climate.*, **6**, 1587-1606.

Konor C. S. , G. Cazes Boezio, C. R. Mechoso and A. Arakawa, 2004: Evaluation of a new PBL parameterization with emphasis in surface fluxes, Proceedings of the 13th AMS Conference on Air-Sea interactions, Portland, Maine.

Konor C. S. and A. Arakawa, 2005: Incorporation of moist processes and a PBL parameterization into the generalized vertical coordinate model. Technical Report No. 102, Department of Atmospheric Sciences, University of California, Los Angeles, 405 Hilgard Ave. 90035, Los Angeles, CA, USA. Available at www.atmos.ucla.edu/~csk.

Ma, C.-C., C. R. Mechoso, A. W. Robertson and A. Arakawa, 1996: Peruvian stratus clouds and the tropical Pacific circulation - a coupled ocean-atmosphere GCM study. *J. Climate*, **9**, 1635-1645.

Mechoso, C. R., J.-Y. Yu and A. Arakawa, 2000: A coupled GCM pilgrimage: From Mechoso, C. R., and Coauthors, 1995: The seasonal cycle over the tropical Pacific in coupled ocean–atmosphere general circulation models. *Mon. Wea. Rev.,* **123,** 2825–2838.

climate catastrophe to ENSO simulations. General circulation model development: Past, present and future. Proceedings of a Symposium in Honor of Professor Akio Arakawa, D. A. Randall, Ed., Academic Press, pp. 539-575.

Pan, D.-M., and D. A. Randall, 1998: A cumulus parameterization with a prognostic closure. *Quart. J. Roy. Meteor. Soc.*, **124**, 949-981.

Randal D. A. and W. H. Schubert, 2004: Dreams of a stratocumulus sleeper. In Atmospheric Turbulence and Mesoscale Meterology, Scientific Research inspired by Douglas Lilly, E. fedorovich, R. Rotuno and B. Stevens (eds.), Cambridge University Press.

Suarez, M. J., A. Arakawa and D. A. Randall, 1983: The parameterization of the planetary boundary layer in the UCLA general circulation model: Formulation and results. *Mon. Wea. Rev.*, **111**, 2224-2243

Yu J. Y. and C. R. Mechoso. 1999: A discussion on the errors in the surface heat fluxes simulated by a coupled GCM. *J. Climate*: Vol. 12, No. 2, pp. 416–426.